Comparison of Performance Effectiveness of Linear Control Algorithms Developed for a Simplified Ground Vehicle Suspension System

by Ross Brown, Jason Pusey, Muthuvel Murugan, and Dy Le

NOTICES

Disclaimers

The findings in this report are not to be construed as an official Department of the Army position unless so designated by other authorized documents.

Citation of manufacturer's or trade names does not constitute an official endorsement or approval of the use thereof.

Destroy this report when it is no longer needed. Do not return it to the originator.

Army Research Laboratory

Aberdeen Proving Ground, MD 21005

ARL-TR-5524   April 2011

Comparison of Performance Effectiveness of Linear Control Algorithms Developed for a Simplified Ground Vehicle Suspension System

Ross Brown
Motile Robotics, Inc, research contractor at U.S. ARL

and

Jason Pusey, Muthuvel Murugan, and Dy Le
Vehicle Technology Directorate, ARL

REPORT DOCUMENTATION PAGE

Form Approved
OMB No. 0704-0188

Public reporting burden for this collection of information is estimated to average 1 hour per response, including the time for reviewing instructions, searching existing data sources, gathering and maintaining the data needed, and completing and reviewing the collection information   Send comments regarding this burden estimate or any other aspect of this collection of information, including suggestions for reducing the burden, to Department of Defense, Washington Headquarters Services, Directorate for Information Operations and Reports (0704-0188), 1215 Jefferson Davis Highway, Suite 1204, Arlington, VA 22202-4302 Respondents should be aware that notwithstanding any other provision of law, no person shall be subject to any penalty for failing to comply with a collection of information if it does not display a currently valid OMB control number

PLEASE DO NOT RETURN YOUR FORM TO THE ABOVE ADDRESS.

1. REPORT DATE *(DD-MM-YYYY)*	2. REPORT TYPE	3. DATES COVERED *(From - To)*
April 2011	Final	FY2010

4. TITLE AND SUBTITLE

Comparison of Performance Effectiveness of Linear Control Algorithms Developed for a Simplified Ground Vehicle Suspension System

5a. CONTRACT NUMBER

5b. GRANT NUMBER

5c. PROGRAM ELEMENT NUMBER

6. AUTHOR(S)

Ross Brown*‡, Jason Pusey, Muthuvel Murugan, and Dy Le

5d. PROJECT NUMBER

5e. TASK NUMBER

5f. WORK UNIT NUMBER

7. PERFORMING ORGANIZATION NAME(S) AND ADDRESS(ES)

Motile Robotics, Inc.
1809 Fashion Ct. Suite 107
Joppa, MD 21085

U.S. Army Research Laboratory
ATTN: RDRL-VTA
Aberdeen Proving Ground, MD 21005

8. PERFORMING ORGANIZATION REPORT NUMBER

ARL-TR-5524

9. SPONSORING/MONITORING AGENCY NAME(S) AND ADDRESS(ES)

10. SPONSOR/MONITOR'S ACRONYM(S)

11. SPONSOR/MONITOR'S REPORT NUMBER(S)

12. DISTRIBUTION/AVAILABILITY STATEMENT

Approved for public release; distribution unlimited.

13. SUPPLEMENTARY NOTES

*Motile Robotics, Inc, research contractor at U.S. ARL
‡ Lead author/Corresponding author, ross.k.brown@us.army mil

14. ABSTRACT

This report documents our evaluation of the effectiveness of active control algorithms in a simulation environment. Each control algorithm was applied to an identical model subjected to the same disturbance input and compared to a baseline passive suspension system and each other algorithm. The control algorithms considered include a Generalized Predictive Controller (GPC) with Implicit Disturbances, GPC with Explicit Disturbances, Linear Quadratic Controller (LQR) and LQR with Preview Control. The suspension model used was a two-degree-of-freedom (2 DOF) quarter car with two sets of vehicle parameters.

15. SUBJECT TERMS

Active suspension, preview control, generalized predictive control

16. SECURITY CLASSIFICATION OF:			17. LIMITATION OF ABSTRACT	18. NUMBER OF PAGES	19a. NAME OF RESPONSIBLE PERSON Ross Brown
a. REPORT	**b. ABSTRACT**	**c. THIS PAGE**	UU	42	19b. TELEPHONE NUMBER *(Include area code)*
Unclassified	Unclassified	Unclassified			(410) 278-0542

Standard Form 298 (Rev. 8/98)
Prescribed by ANSI Std. Z39.18

Contents

List of Figures

List of Tables

1. Summary

This report discusses the research conducted by the U.S. Army Research Laboratory, Vehicle Technology Directorate (ARL-VTD) on advanced suspension control. ARL-VTD research on advanced suspension systems should result in a reduction of ground vehicle chassis vibration while maintaining tire contact with the road surface. The purpose of this research is to reduce vibration-induced fatigue to the Warfighter, as well as to improve the gun shooting precision.

2. Introduction

Passive suspension systems for ground vehicles are optimized for passenger comfort or road/terrain handling. Quite often these two goals contradict each other. Modern suspension systems may include control systems that use sensors and actuators to improve both performance metrics at the expense of increased complexity and cost.

The two main groups of advanced suspension systems are divided into fully-active and semi-active actuators. Semi-active suspension systems vary spring and damper properties to store or remove energy from the system according to the applied control algorithm. Most commonly, this is achieved through variable damping components: variable orifice valves or magneto-rheological (MR) fluids. Fully-active suspension systems use actuators to add and remove energy from the system. This is achieved using hydraulic, pneumatic, or electromechanical actuators. This report focuses on fully-active actuator control algorithms.

The baseline control algorithm for this research is the Linear Quadratic Regulator (LQR). This algorithm has been extended to incorporate future road profile disturbance data through Preview Control. Another algorithm, Generalized Predictive Control, was evaluated with formulations for Implicit Disturbances and Explicit Disturbances. Generalized Predictive Control with Preview Control was not considered in this completed research work. This will be considered in future research.

3. Modeling and Simulation

Two primary vehicle models were developed in Mathworks Matlab-Simulink to gain insight into the behavior of the vehicle's suspension subject to various road conditions. These models were idealized representations of a quarter of the vehicle. The models were implemented in Mathworks Matlab/Simulink for simulation.

The Quarter Car, as shown in figure 1, is modeled as 25% of the chassis mass riding on a suspension system consisting of a spring, damper, and actuator. This is connected to the wheel, which is modeled as a lumped mass with a very stiff spring and very soft damper. Road disturbance is introduced through the wheel suspension system. The control actuator is treated as a perfect force generator; thus, there are no dynamics associated with the actuator model.
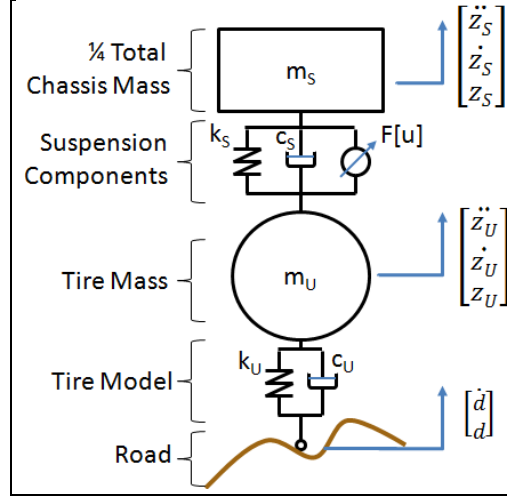

Figure 1. Quarter-car suspension model.

In the representative model shown above, the lumped masses each have a single degree-of-freedom - vertical motion of the mass centroid; therefore, this is a two-degree-of-freedom (2 DOF) system. This system is then modeled as a system of second order differential equations. In this linearized model, two assumptions must be noted:

(1) The tire always remains in contact with the ground, and

(2) There are no stroke limits for the suspension components.

$$\begin{bmatrix} \frac{m_S}{4} & & & \\ & m_U & & \\ & & 1 & \\ & & & 1 \end{bmatrix} \begin{bmatrix} \ddot{z}_S \\ \ddot{z}_U \\ \dot{z}_S \\ \dot{z}_U \end{bmatrix} = \begin{bmatrix} -C_S & C_S & -K_S & K_S \\ C_S & -C_S - C_U & K_S & -K_S - K_U \\ 1 & & & \\ & 1 & & \end{bmatrix} \begin{bmatrix} \dot{z}_S \\ \dot{z}_U \\ z_S \\ z_U \end{bmatrix} + \begin{bmatrix} F \\ -F \\ \\ \end{bmatrix} [u] + \begin{bmatrix} C_U & K_U \\ \\ \end{bmatrix} \begin{bmatrix} \dot{d} \\ d \end{bmatrix}$$

$$[\dot{x}] = A [x] + B_c [u] + B_d [d]$$

where

[x] is the state vector comprised of: z_U, z_S, $\dot{z}_U$, and $\dot{z}_S$,

z_U is the height of the tire centroid above a starting reference zero,

z_S is the height of the chassis centroid above a starting reference zero,

$\dot{z}_U$ is the vertical velocity of the tire,

$\dot{z}_S$ is the vertical velocity of the vehicle chassis

2

[u] is the control vector comprised of each control actuator

[d] is the disturbance vector comprised of: d, and $\dot{d}$,

Subscript c indicates the control component of the input matrix, and

Subscript d indicates the disturbance component of the input matrix

The particular parameters chosen for each component in the Quarter Car modeled are listed in tables 1 and 2. These are taken from two papers discussing recent active control research. The two sets of vehicle parameters will be referred to as *Light Vehicle* (*2*) and *Heavy Vehicle* (*3*). These models are used to reproduce data for the control systems in this report. This provides a common reference point for comparison of the control algorithms; these do not necessarily represent parameters for a specific vehicle.

Table 1. *Light Vehicle* Parameters used in research by El Madany, et al., (*2*).

Vehicle Parameters – Light Vehicle		
m_S	1155.6 kg	total chassis (sprung) mass
m_U	28.58 kg	tire (unsprung) mass
K_S	19960 $^N/_m$	suspension spring rate[*]
C_S	816.46 $^{Ns}/_m$	suspension damping[*]
K_U	155900 $^N/_m$	tire spring rate
C_U	0 $^{Ns}/_m$	tire damping
1st mode	1.237 Hz	chassis natural frequency
2nd mode	12.15 Hz	tire natural frequency
[*]stiffness and damping chosen to provide damping ratio of 0.17		

Table 2. *Heavy Vehicle* parameters used in algorithm research by van der Aa, et al., (*3*).

Vehicle Parameters – Heavy Vehicle		
m_S	34600 kg	total chassis (sprung) mass
m_U	1350 kg	tire (unsprung) mass
K_S	440000 $^N/_m$	suspension spring rate
C_S	43100 $^{Ns}/_m$	suspension damping
K_U	6500000 $^N/_m$	tire spring rate
C_U	0 $^{Ns}/_m$	tire damping
1st mode	1.055 Hz	chassis natural frequency
2nd mode	10.95 Hz	tire natural frequency

4. Controller Methodology

Several different controllers were considered and employed on the suspension models developed. The performance of the controllers was evaluated against each other with the passive suspension model as the baseline. These algorithms are multi-input/multi-output controllers. Thus, the control command, $[u_t]$, can be a vector where each element corresponds to a value of a specific

actuator at time t. The same is applicable for the measured response, $[y_t]$, and external disturbances, $[d_t]$.

All of the algorithms discussed in this research are classified as *optimal control algorithms.* Optimal control algorithms calculate a control command that best satisfy a specified *objective function.* The objective function is often a linear combination of weighted state-vectors, measured responses, and control commands integrated. The minimum of the objective function, found by setting the derivative of the objective function to zero, corresponds to the optimum command. The weighting matrices serve two purposes. First, they are used to normalize and non-dimensionalize the input/output data. Thus, large accelerations and small displacements can be used to provide a dimensionless objective function. The second purpose of the weighting matrices is that they allow relative performance penalties. For example, high accelerations in the crew cabin should be penalized more than the same level of acceleration in the cargo bay.

These algorithms are formulated as *regulators. Regulator Control* derives the control command required to drive the feedback inputs to zero. Conversely, *Tracking Control* drives the feedback inputs to follow a specified path. *Deadbeat Regulator Control* derives the control command such that for a discrete-time model the closed loop poles are zero in the complex plane; thus, the closed loop system is critically damped.

Two other concepts are applicable to algorithms in this research. *Preview Control* or *Look-Ahead Control* measures the external disturbance before it affects the vehicle and incorporates this information into the control algorithms. LQR with Preview Control is discussed below. *System Identification* is a process where an algorithm identifies the vehicle model based on a history of measured inputs and outputs. Various control laws can then be calculated and applied to the vehicle. Generalize Predictive Control algorithms perform a system identification on the fly to calculate the control laws.

4.1 LQR

Linear Quadratic Regulator is the most basic of the optimal control algorithms. This control algorithm is a full-state feedback controller. Given a perfect model of the vehicle dynamics, the optimal control command can be calculated and applied. Full-state feedback requires that every state in the model can be measured and fed into the control law.

Recall the state space model of the vehicle dynamics from the previous section:

$$[\dot{x}] = A\,[x] + B_c[u] + B_d[d]$$

For LQR, the control command is calculated as a matrix gain multiplied by the state-vector. Thus, the control command, u, is calculated by

$$[u] = -K[x],$$

where

K is the LQR feedback matrix gain, and

$[x]$ is the state vector.

The feedback matrix gain is obtained by building a quadratic objective function, J, and solving for the minimum:

$$J = \int_0^\infty (x^T Q x + u^T R u + 2 x^T N u) \partial t$$

where

Q is a symmetric positive semi-definite matrix that assigns weights to the state vector,

R is a symmetric positive definite matrix that assigns weights on the control commands,

N is a symmetric positive semi-definite matrix that assigns weights for the cross-coupled terms. N is often assumed to be null.

The superscript T indicates the vector or matrix transpose

The minimum is obtained by taking the derivative of the function and setting it equal to zero.

$$0 = \frac{\partial J}{\partial t} = x^T Q x + u^T R u + 2 x^T N u$$

The equation devolves into an Algebraic Riccati Equation (ARE), and the LQR feedback gain matrix is calculated from

$$K = R^{-1} B_C^T P,$$

where P is the solution to the ARE.

As implemented in this research, LQR feedback control is formulated for discrete time domain.

4.2   LQR with Preview Control

Linear Quadratic Regulator with Preview Control extends the LQR with an additional control command component based on future disturbance data. Preview Control was first published by Bender (*1*), and is further developed in papers by El Madany, et al., (*2*) and van der Aa, et al., (*3*).

The closed loop state matrix is used to calculate the optimal command for each disturbance in the future. The resulting commands are integrated to provide a weighted augmentation to the LQR closed loop control command, as shown below:

$$[u] = -K[x] - R^{-1} B_C^T \int_t^{t + t_{Preview}} \left(e^{(A - B_C K)} \right) \partial t,$$

where the preview horizon, $t_{Preview}$, is the time that corresponds to the furthest valid future disturbance data point.

The number of samples of future disturbance can be varied based on the capability of the sensor and vehicle ground speed. Again, for this research, this control algorithm was formulated in discrete time domain. Performance of the control system for the chosen number of Preview samples was compared.

4.3 GPC with Implicit Disturbance

Generalized Predictive Controller (GPC), as detailed in a paper by Kvaternik, et al., (4) and the text by Juang (5), is a linear, time-invariant, multi-input/multi-output controller that generates an Autoregressive with Exogenenous (ARX) model. This means that GPC builds a time-domain based model from time-history data of measured responses and control commands. This ARX model is used to derive a control law that implements an optimal deadbeat regulator. GPC is capable of performing this system identification and control law generating the model in near-real-time. The system identification portion requires that the controller inject frequency-rich control commands into the system, typically band-limited white noise (random signal with a flat power spectral density). The issued commands and resulting system responses are used to build the ARX model. External disturbances are not directly measured and are implicitly accounted for in the measured responses.

The first step in performing *System Identification* and model calculation is to inject the independent white noise signals into all of the control actuators. This will generate an *l*-sample input/output time history of measured responses, *y*, and generated commands, *u*. These samples are arrayed into the input/output data matrix, *V*.

$$V = \begin{bmatrix} u_{t-0} & u_{t-1} & u_{t-2} & \cdots & u_{t-p} & \cdots & u_{t-l+1} \\ & u_{t-0} & u_{t-1} & \cdots & u_{t-p+1} & \cdots & u_{t-l+2} \\ & y_{t-0} & y_{t-1} & \cdots & y_{t-p+1} & \cdots & y_{t-l+2} \\ & & u_{t-0} & \cdots & u_{t-p+2} & \cdots & u_{t-l+3} \\ & & y_{t-0} & \cdots & y_{t-p+2} & \cdots & u_{t-l+3} \\ & & & \ddots & \vdots & \cdots & \vdots \\ & & & & u_{t-0} & \cdots & u_{t-l+p+1} \\ & & & & y_{t-0} & \cdots & y_{t-l+p+1} \end{bmatrix}$$

Given this matrix, the observer Markov parameters, $\bar{Y}$, can be calculated with the following equation:

$$y = \bar{Y}V$$

$$\begin{bmatrix} y_{t-0} \\ \vdots \\ y_{t-l} \end{bmatrix} = \bar{Y} \begin{bmatrix} u_{t-0} & u_{t-1} & u_{t-2} & \cdots & u_{t-p} & \cdots & u_{t-l+1} \\ & u_{t-0} & u_{t-1} & \cdots & u_{t-p+1} & \cdots & u_{t-l+2} \\ & y_{t-0} & y_{t-1} & \cdots & y_{t-p+1} & \cdots & y_{t-l+2} \\ & & u_{t-0} & \cdots & u_{t-p+2} & \cdots & u_{t-l+3} \\ & & y_{t-0} & \cdots & y_{t-p+2} & \cdots & u_{t-l+3} \\ & & & \ddots & \vdots & \cdots & \vdots \\ & & & & u_{t-0} & \cdots & u_{t-l+p+1} \\ & & & & y_{t-0} & \cdots & y_{t-l+p+1} \end{bmatrix}$$

Solve for $\bar{Y}$ by applying the psuedoinverse to V. The columns of $\bar{Y}$ can be rearranged to provide the multi-step output predictor.

$$\bar{Y} = [\tau \quad \beta_1 \quad \alpha_1 \quad \beta_2 \quad \alpha_2 \quad \cdots \quad \beta_p \quad \alpha_p]$$

The resulting vehicle model is a weighted sum of the time history data. This can be used to predict the future responses given the past history and future commands.

$$[y_p] = \tau[u_p] + \alpha[y_p] + \beta[u_p]$$

$$\begin{bmatrix} y_{t+0} \\ \vdots \\ y_{t+p} \end{bmatrix} = \tau \begin{bmatrix} u_{t+0} \\ \vdots \\ u_{t+p} \end{bmatrix} + \alpha \begin{bmatrix} y_{t-1} \\ \vdots \\ y_{t-p} \end{bmatrix} + \beta \begin{bmatrix} u_{t-1} \\ \vdots \\ u_{t-p} \end{bmatrix}$$

The next predicted response is the first row of the previous equation

$$y_{t+0} = \tau u_{t+0} + \alpha_1 y_{t-1} + \beta_1 u_{t-1} + \cdots + \alpha_p y_{t-p} + \beta_p u_{t-p}$$

As with LQR, a control law can be designed based on an objective function,

$$J = \int_0^\infty (y^T Q y + u^T R u)\partial t$$

Substituting the expanded equation for $[y]$ yields

$$J = \int_0^\infty \left(\left[\tau \begin{bmatrix} u_{t+0} \\ \vdots \\ u_{t+p} \end{bmatrix} + \alpha \begin{bmatrix} y_{t-1} \\ \vdots \\ y_{t-p} \end{bmatrix} + \beta \begin{bmatrix} u_{t-1} \\ \vdots \\ u_{t-p} \end{bmatrix} \right]^T Q \left[\tau \begin{bmatrix} u_{t+0} \\ \vdots \\ u_{t+p} \end{bmatrix} + \alpha \begin{bmatrix} y_{t-1} \\ \vdots \\ y_{t-p} \end{bmatrix} + \beta \begin{bmatrix} u_{t-1} \\ \vdots \\ u_{t-p} \end{bmatrix} \right] + u^T R u \right)\partial t$$

Finding the local minimum of the objective function, J, yields an optimal solution for the control commands that minimize the responses. Taking the partial derivative with respect to command, $[u]$, and solving for control commands, yields the following:

$$\begin{bmatrix} u_{t+0} \\ \vdots \\ u_{t+p} \end{bmatrix} = -(\tau^T R \tau + Q)^{-1}\tau^T R \left[\alpha \begin{bmatrix} y_{t-1} \\ \vdots \\ y_{t-p} \end{bmatrix} + \beta \begin{bmatrix} u_{t-1} \\ \vdots \\ u_{t-p} \end{bmatrix} \right]$$

Defining the following control law matrices,

$$\alpha_C = -(\tau^T R \tau + Q)^{-1}\tau^T R \alpha,$$

$$\beta_C = -(\tau^T R \tau + Q)^{-1}\tau^T R \beta,$$

yields control laws that calculate the next p commands,

$$\begin{bmatrix} u_{t+0} \\ \vdots \\ u_{t+p} \end{bmatrix} = \alpha_C \begin{bmatrix} y_{t-1} \\ \vdots \\ y_{t-p} \end{bmatrix} + \beta_C \begin{bmatrix} u_{t-1} \\ \vdots \\ u_{t-p} \end{bmatrix},$$

where u_{t+p} corresponds to the control commands p steps into the future.

However, only the next control commands are of interest, thus the rows of $[u]$ corresponding to future data can be dropped.

$$[u_{t+0}] = \bar{\alpha}_C \begin{bmatrix} y_{t-1} \\ \vdots \\ y_{t-p} \end{bmatrix} + \bar{\beta}_C \begin{bmatrix} u_{t-1} \\ \vdots \\ u_{t-p} \end{bmatrix}$$

4.4   GPC with Explicit Disturbance

Generalized Predictive Controller with Explicit Disturbance, as described in a subsequent publication by Kvaternik, et al. (*6*), is similar to the previous version of GPC, except that now the external disturbances are explicitly modeled. Time histories of controls commands, measurement responses, and, now, disturbance measurements are used to generate the ARX model for the system.

$$\bar{Y} = [\gamma \quad \tau \quad \delta_1 \quad \beta_1 \quad \alpha_1 \quad \delta_2 \quad \beta_2 \quad \alpha_2 \quad \dots \quad \delta_p \quad \beta_p \quad \alpha_p]$$

These are used to predict future responses based on past responses (including external disturbances) and control commands. In this formulation, it is assumed that the current disturbance can be measured.

$$[y_p] = \tau[u_p] + \alpha[y_p] + \beta[u_p] + \delta[d_p]$$

$$\begin{bmatrix} y_{t+0} \\ \vdots \\ y_{t+p} \end{bmatrix} = \tau \begin{bmatrix} u_{t+0} \\ \vdots \\ u_{t+p} \end{bmatrix} + \alpha \begin{bmatrix} y_{t-1} \\ \vdots \\ y_{t-p} \end{bmatrix} + \beta \begin{bmatrix} u_{t-1} \\ \vdots \\ u_{t-p} \end{bmatrix} + \delta \begin{bmatrix} d_{t-1} \\ \vdots \\ d_{t-p} \end{bmatrix}$$

As before, the next control commands are calculated by minimizing the objective function; the rows corresponding to future control commands are dropped. Using this extension, the previous measured disturbance information can be used.

---

5.   Road Profiles

Three road profiles were used to evaluate the algorithms: Sine, Curb, and Perryman 3. In each case, the road profiles were provided as an array of ground distance and vertical heights. Vehicle speed was integrated to track the position along the ground and calculate road height at the next time step.

5.1   Sine

This road profile was defined by a sine wave with a half-amplitude of 20 cm with a wavelength of 1 m. The intent was to provide a single frequency disturbance that relates to vehicle speed, in this case, 1 m/s (3.6 kph) of speed corresponds to 1 Hz excitation. Figure 2 shows a portion of this type of road profile.
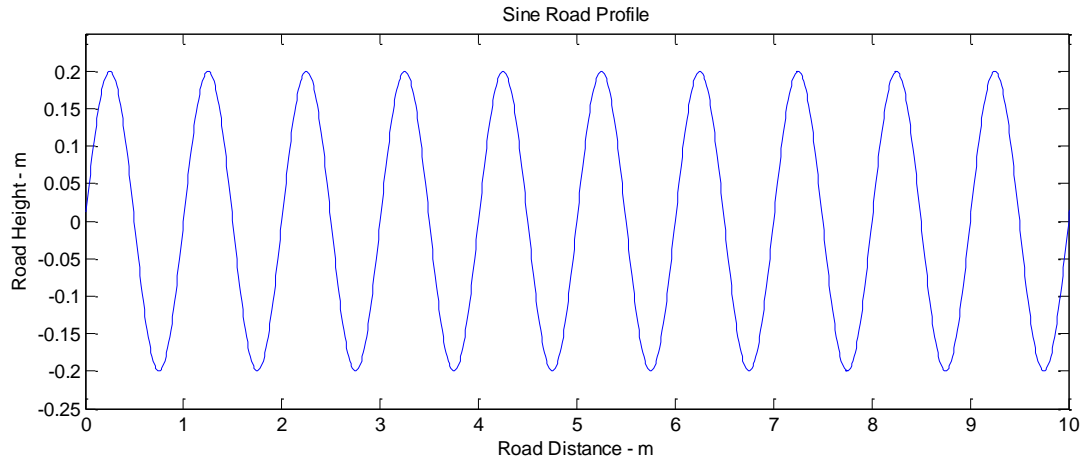
Figure 2. *Sine* road profile.

5.2 Curb

This road profile is defined by a 10 cm step rise followed 50 by meters of level surface, and then a 10 cm step drop. The intent was to provide a step input road profile into the system. Note that the input was modeled as a step input to the tire. It does not accurately take the geometry of a physical tire rolling over curb into account, which would effectively low-pass filter the curb input. Figure 3 shows this road profile.
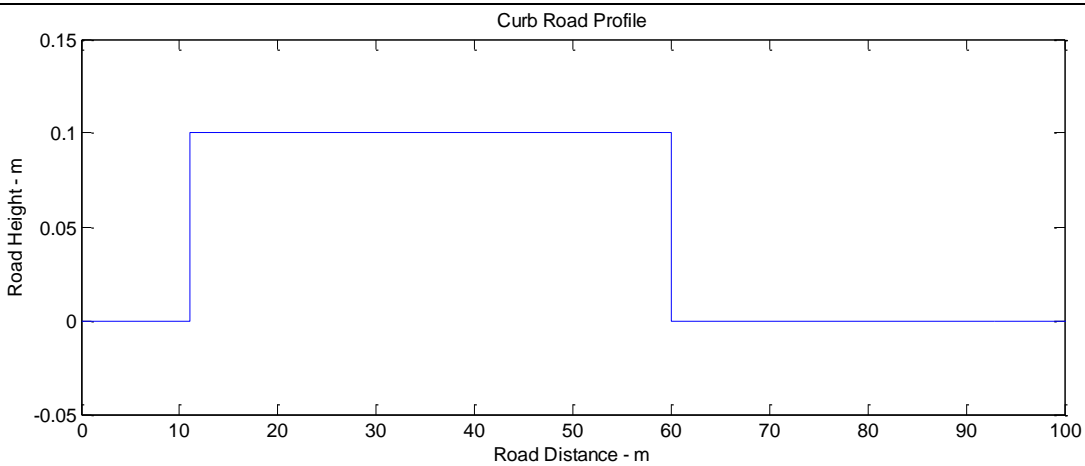

Figure 3. *Curb* road profile.

5.3 Perryman3

Perryman 3 is an off-road test track located at Aberdeen Proving Ground. This road profile is intended to evaluate the algorithms against a challenging, "real-world" course. Figure 4 shows this road profile.
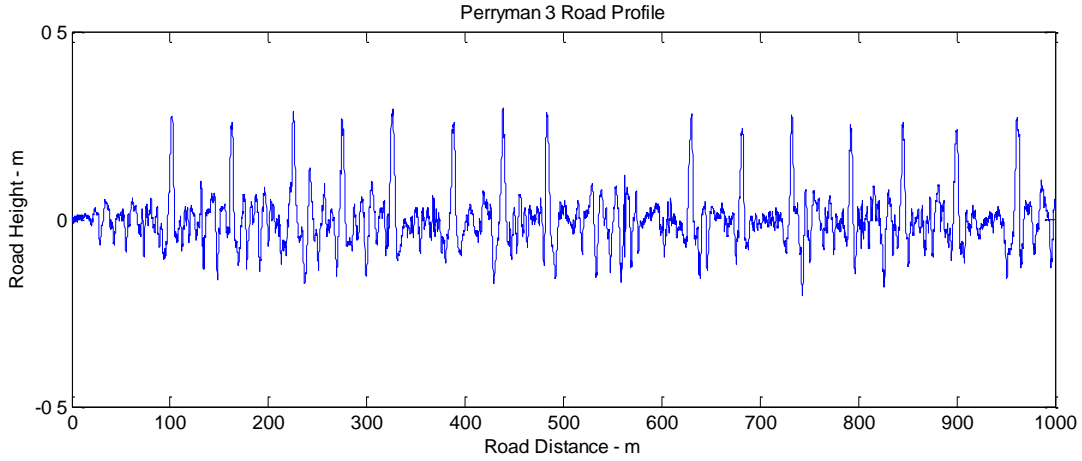
9

Figure 4. *Perryman 3* road profile.

6. Simulation Results

The vehicle models and controllers were implemented in Mathworks Matlab and Simulink. The simulation was run using discrete time steps at 0.01 s (100 Hz) using the ODE5 (Dormand-Prince) integration method. The simulations were run for 12 s until the model reached steady state. The open loop model was run in parallel with closed-loop LQR, closed-loop LQR with Preview Control, GPC with Implicit Disturbances, and GPC with Explicit Disturbances for performance comparison studies. The Preview Control block was pre-populated with the $t_{Preview}$ road profile samples at the start of the simulation.

Initial conditions for the suspension were equal to zero and the effects of gravity were ignored such that the system would be at steady state prior to the addition of external disturbances. Vehicle speed was held at a constant value for the entire run.

The following objective function was used as the metric for comparing algorithm performance

$$J = \ low\ pass(\sqrt{y^T y + u^T u}\ )$$

The values for each simulation were averaged over the 12 s and plotted at multiple vehicle speeds. The measured responses are normalized against the open-loop responses at each speed.

$$Normalized\ Response = 1 - \frac{J_{algorithm}}{J_{open}}$$

The actuator forces and powers are normalized against the baseline algorithm, LQR, R=1.

$$Normalized\ Actuator = \frac{J_{algorithm}}{J_{LQR,R=1}}$$

10

This normalization allows a comparison of the algorithms despite the variation in actuator force or power.

$$Normalized\ Effectiveness = \frac{Normalized\ Response_{\ algorithm}}{Normalized\ Actuator_{algorithm}}$$

6.1 Algorithms

A short comparison of the four control laws operating on two sets of quarter-car parameters and three road courses (disturbance inputs) is presented in the discussion below.

Simulation data based on the *Light Vehicle* parameters is presented in figures 5, 7, and 12. These figures were generated using the following algorithm parameters, as shown in table 3.
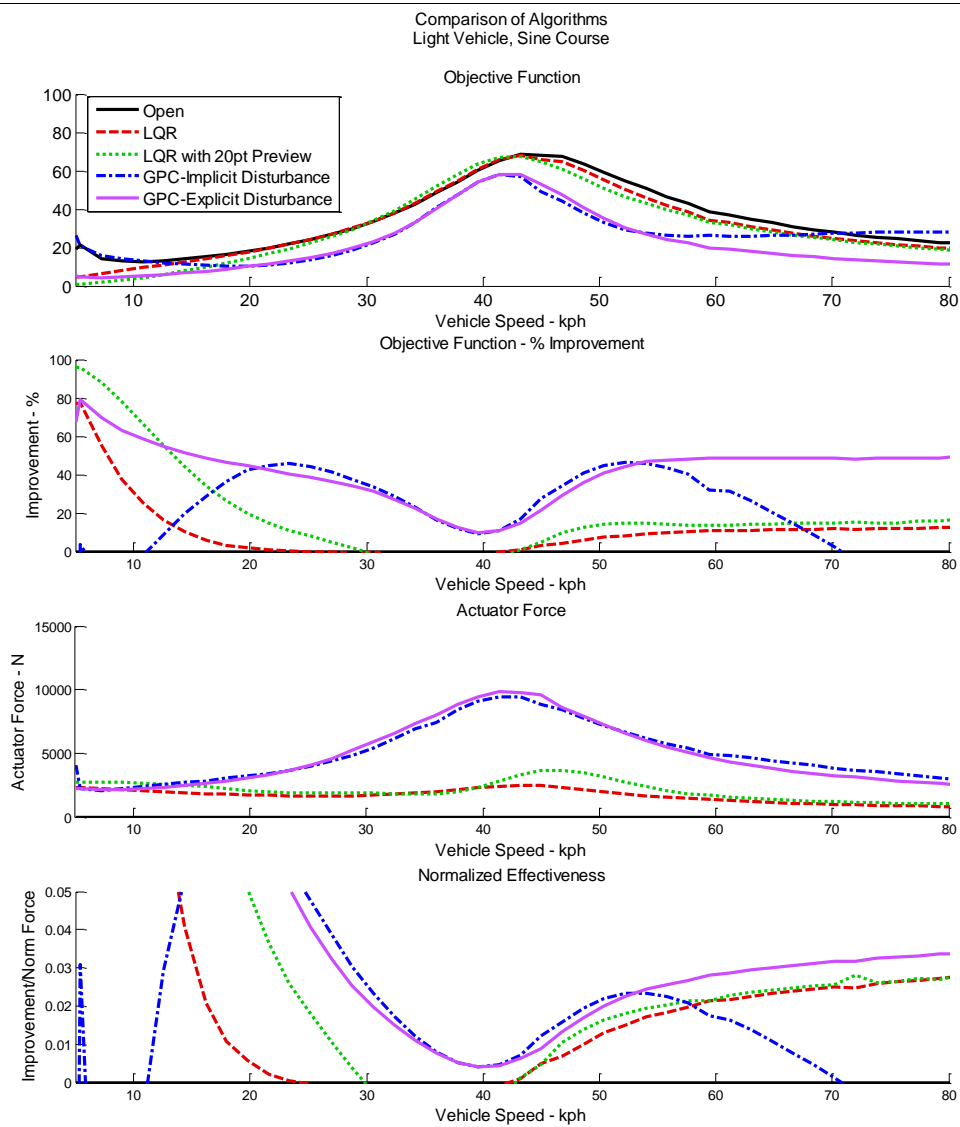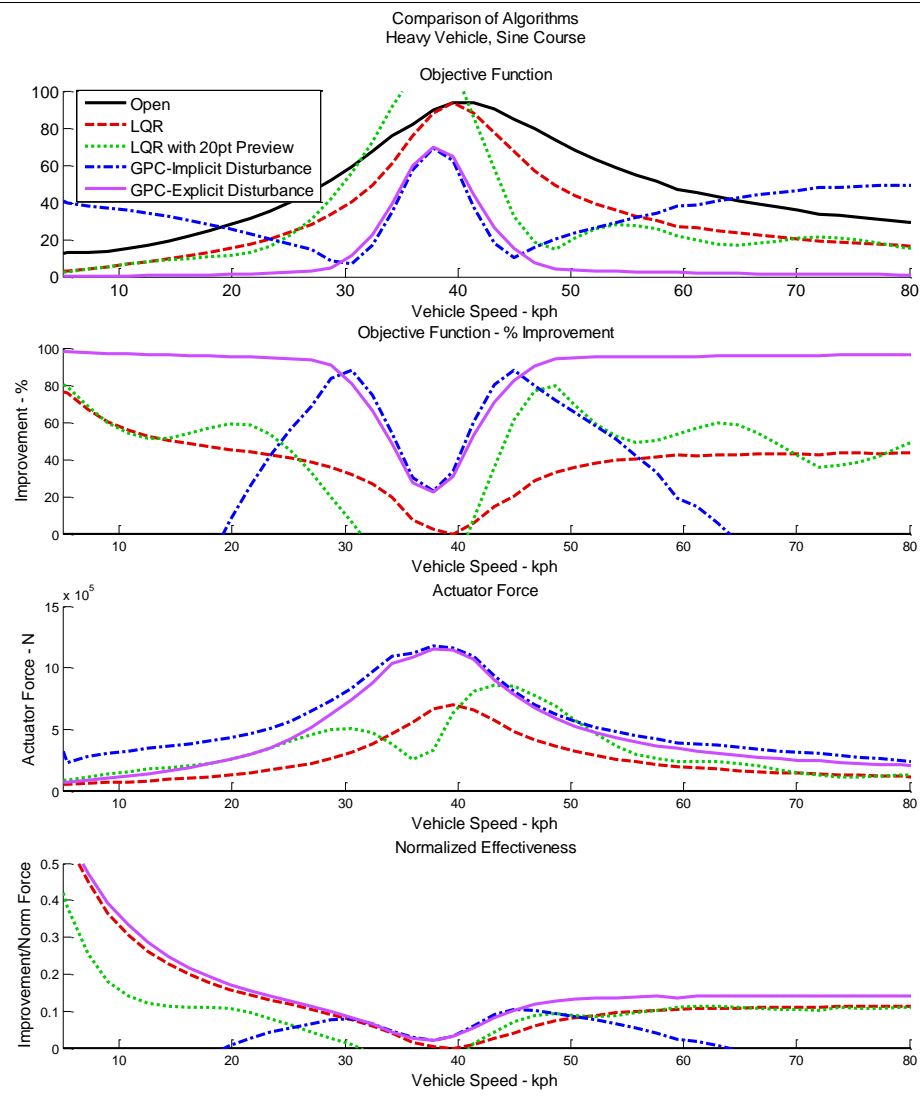

Figure 5. Comparison of control algorithms for *Light Vehicle* parameters on Sine course.

Table 3. Algorithm tuning parameters used for *Light Vehicle* parameters.

	LQR	LQR with Preview Control	GPC with Implicit Disturbance	GPC with Explicit Disturbance
sensors	4 (internal states)	4 (internal states)	3	3
actuators	1			
Q	1e8*[1 0 1 1]	1e8*[1 0 1 1]	1e5*[1 1 1]	1e5*[1 1 1]
R	1	1	1	1
Preview Horizon	-	20 points	-	-
ARX model size	-	-	6	6
ID sample size	-	-	400 points	400 points
ID disturbance	-	-	10 Hz sine	white noise
Actuator Limit	1.5e4 N			

Simulation data using the *Heavy Vehicle* parameters is presented in figures 6, 8, and 13. These figures were generated using the following algorithm parameters, as shown in table 4.

Figure 6. Comparison of control algorithms for *Heavy Vehicle* parameters on Sine course.

Table 4. Algorithm tuning parameters used for *Heavy Vehicle* parameters.

	LQR	LQR with Preview Control	GPC with Implicit Disturbance	GPC with Explicit Disturbance
sensors	4 (internal states)	4 (internal states)	3	3
actuators	1			
Q	1e12*[1 0 1 1]	1e12*[1 0 1 1]	5e9*[1 1 1]	5e9*[1 1 1]
R	1	1	1	1
Preview Horizon	-	20 points	-	-
ARX model size	-	-	6	6
ID sample size	-	-	400 points	400 points
ID disturbance	-	-	10 Hz sine	white noise
Actuator Limit	1.5e6 N			

Figures 5 and 6 correspond to the *Sine* road profile, which represents a single frequency disturbance. In the regions where the control laws are valid, both GPC algorithms show higher performance. Note that the LQR based algorithms actually perform worse than the open loop case near vehicle resonance. Knowledge of disturbance extends the region over which the control laws are valid and effective, as demonstrated by GPC with Explicit Disturbances and LQR with Preview Control.

The performance of the algorithms for the *Curb* road profile is shown in figures 7 and 8.
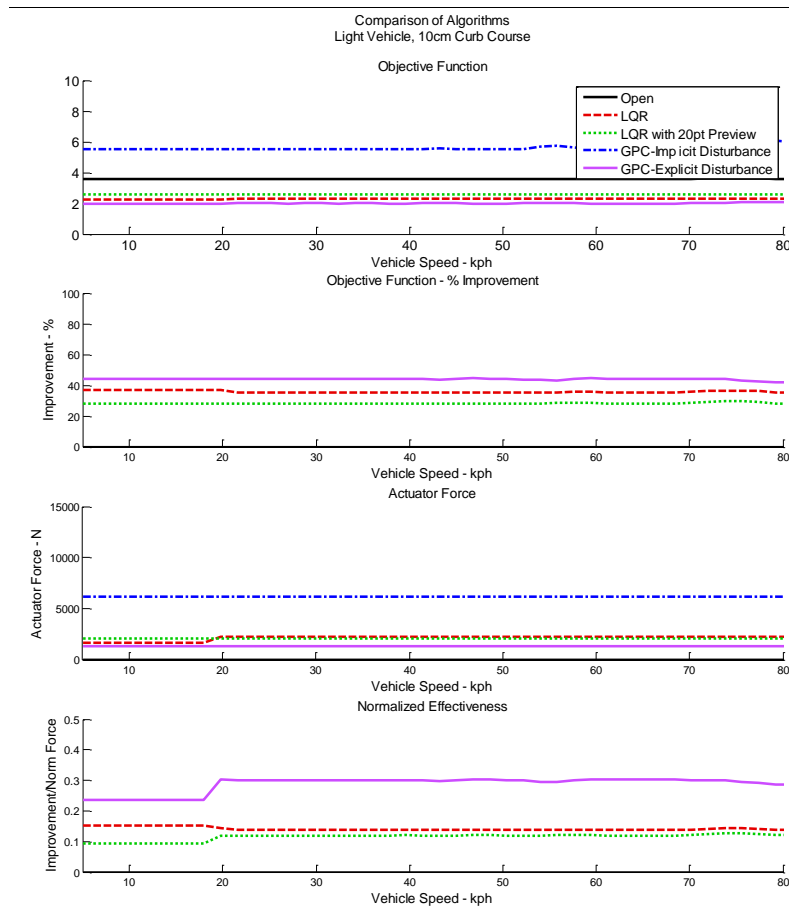

Figure 7. Comparison of control algorithms for *Light Vehicle* parameters on Curb course.
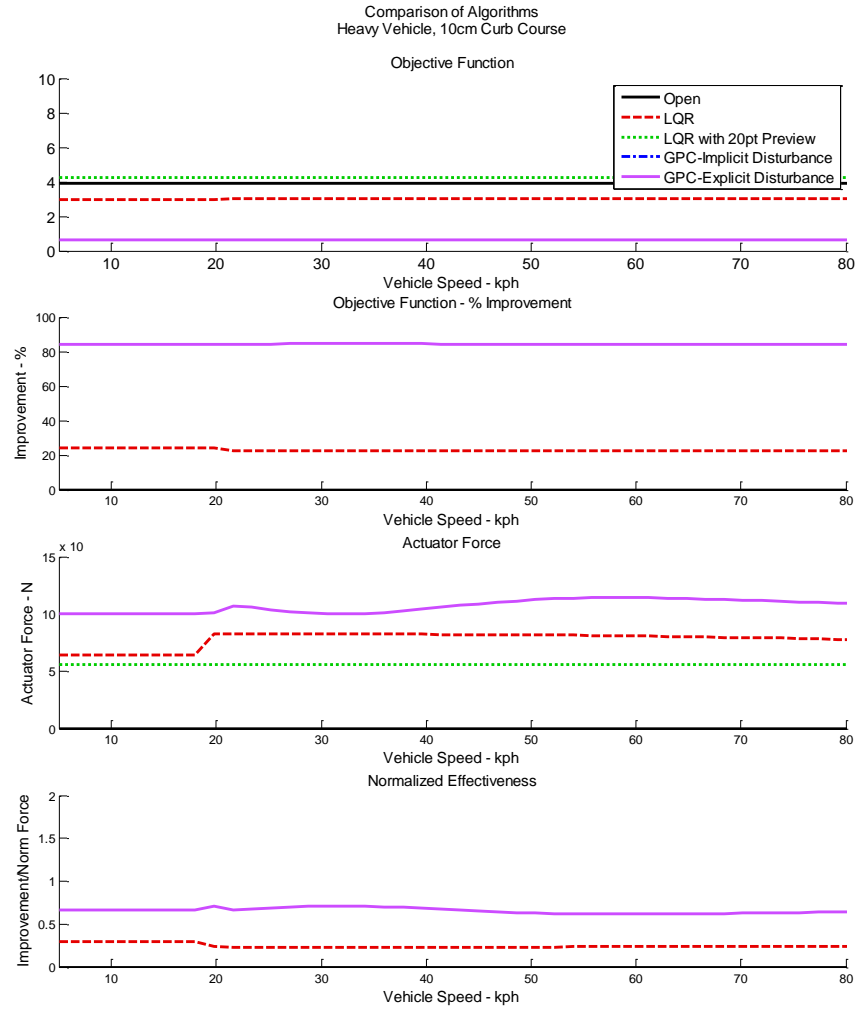
Figure 8. Comparison of control algorithms for *Heavy Vehicle* parameters on Curb course.

GPC with Implicit Disturbance performs much worse than the open loop case as shown in figure 9. This is caused by the fact that the measured value for tire height has a non-zero offset relative to the starting reference height.
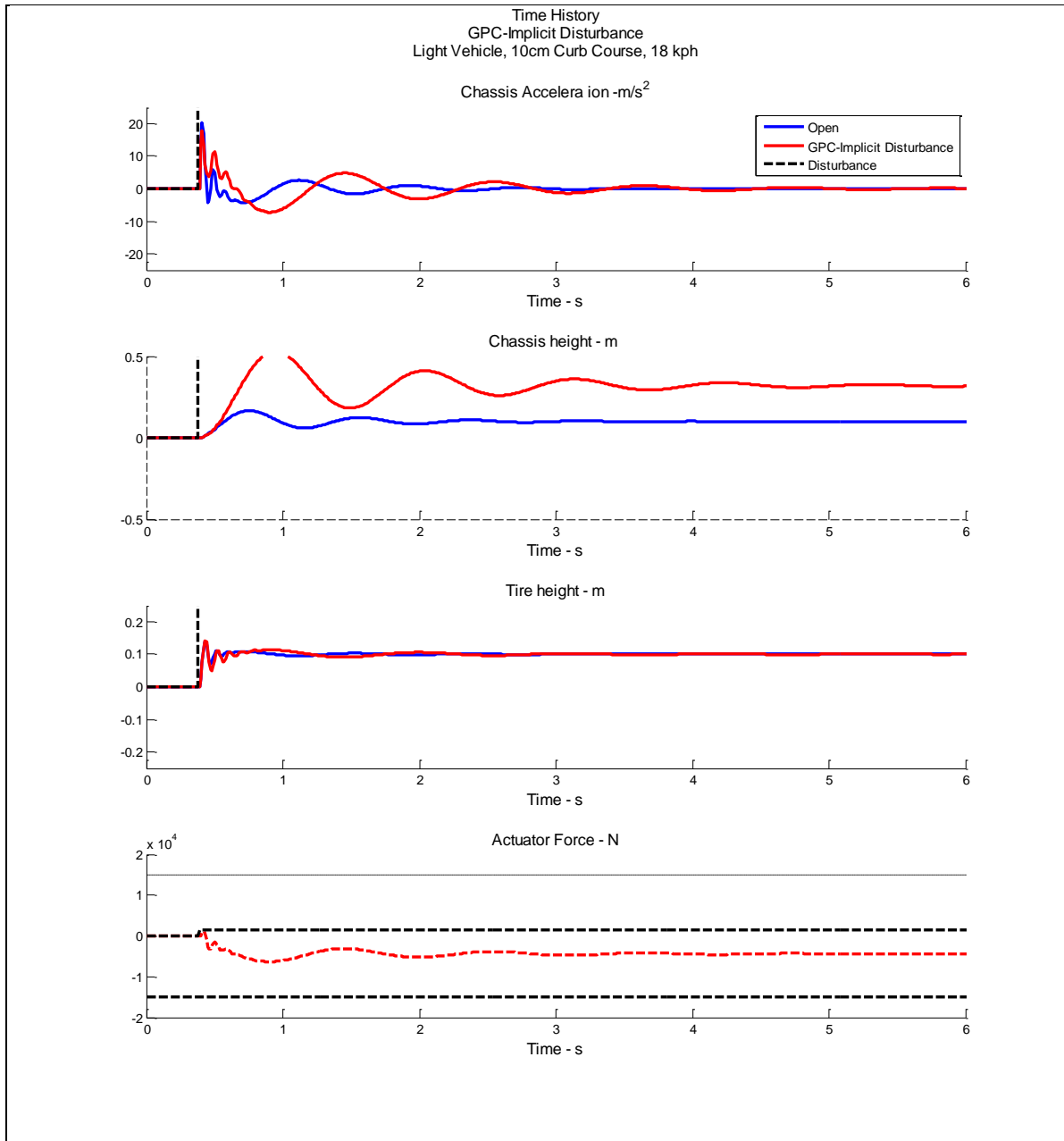
Figure 9. Time history of GPC with implicit disturbance for *Light Vehicle* parameters on Curb course.

LQR with Preview Control also appears to have worse performance than open loop. However, it is clear from figure 10 that it has a much lower settling time. Also, in the case of LQR with Preview Control, special note must be given to the fact that the actuator commands begin well ahead of the disturbance, thus reducing accelerations on the vehicle when encountering the step input, as shown in figure 11. It is inferred from results that vehicle speed is not a major factor in the algorithm performance since the road input ignores the effect of tire geometry rolling up and over the curb.
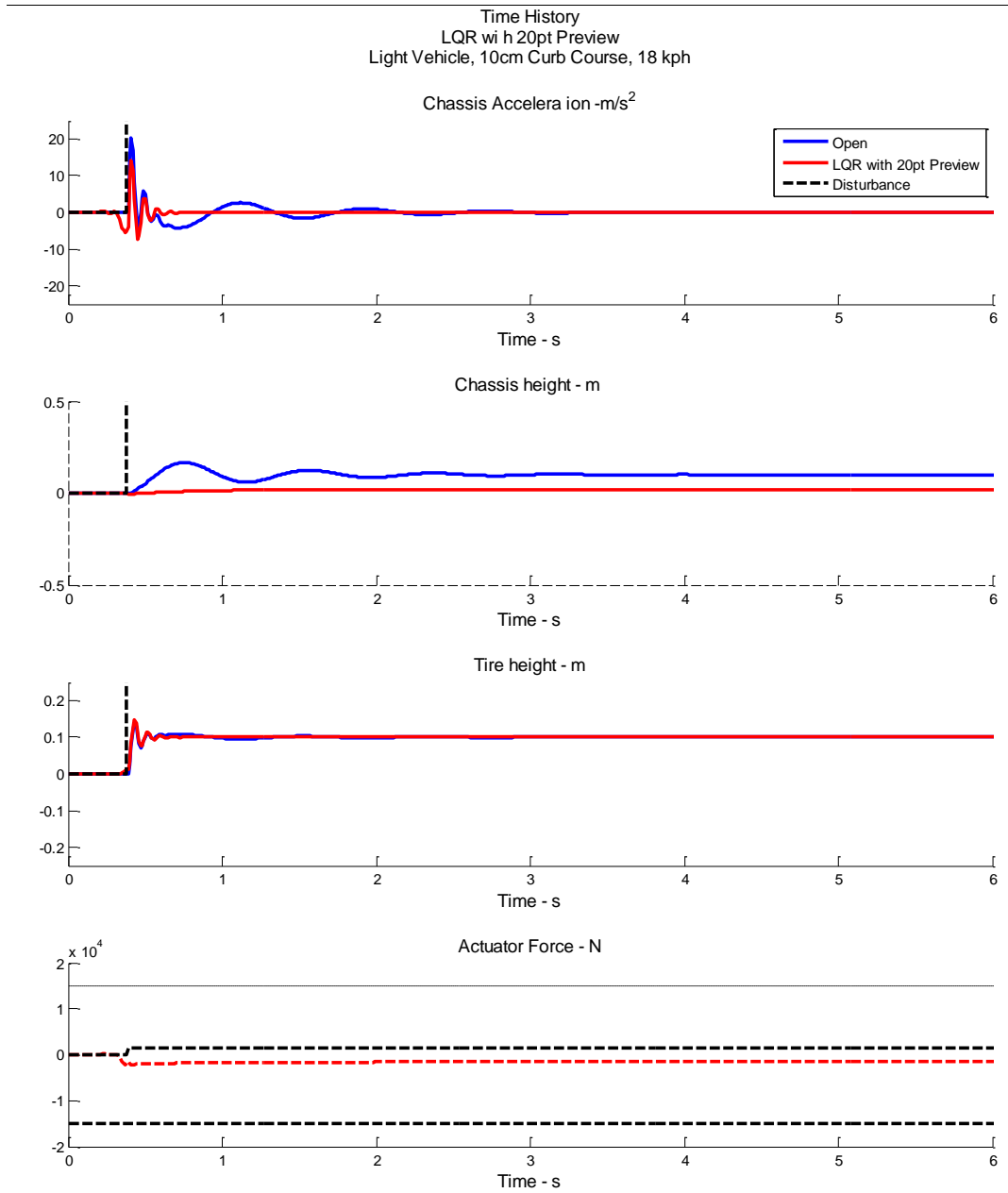
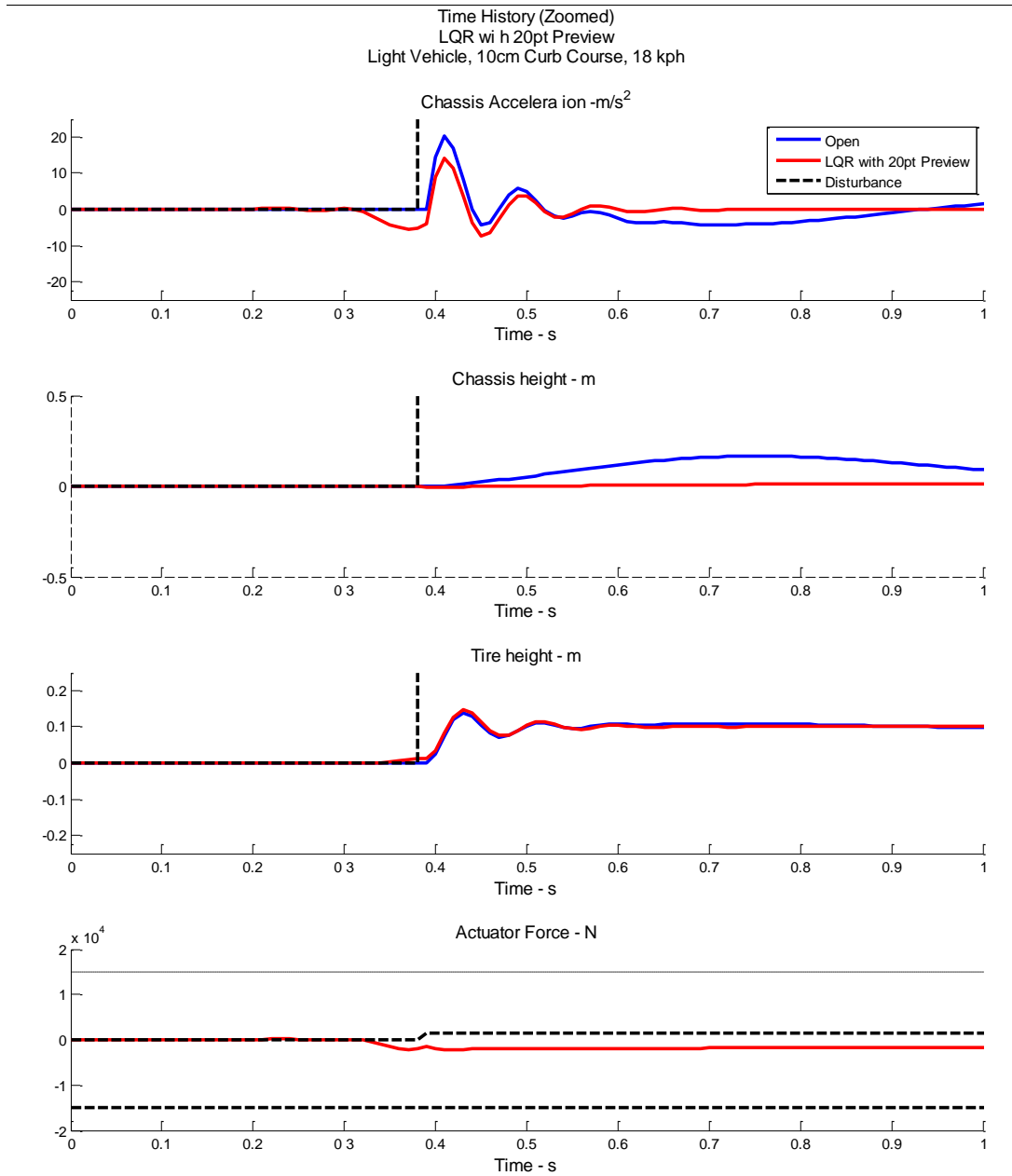Figure 10. Time history of LQR with preview control for *Light Vehicle* parameters on Curb course.

Figure 11. Time history of LQR with preview control, close up of step input.

The results from the final road profile, *Perryman 3*, are shown in figures 12 and 13. Again, GPC with Implicit Disturbance responds poorly to the input. LQR, LQR with Preview Control, and GPC with Explicit Disturbance perform well on this aperiodic road profile. Although the Normalized Effectiveness appears similar for these three algorithms, it is interesting to observe that the objective function for GPC with Explicit Disturbance is relatively flat over the entire frequency range. This suggests that the closed-loop vehicle response will be independent of vehicle speed.
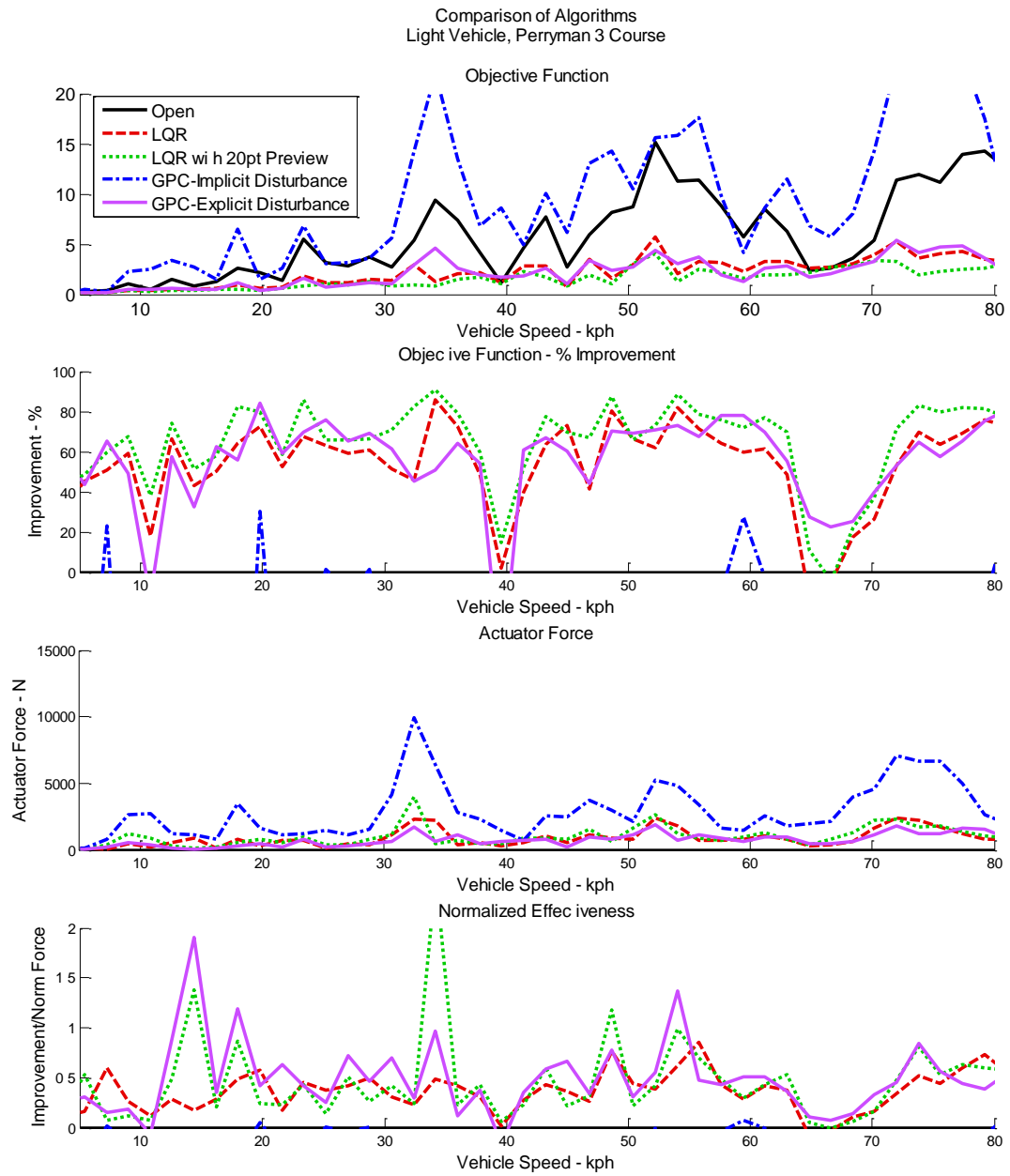
Figure 12. Comparison of control algorithms for *Light Vehicle* parameters on Perryman 3 course.
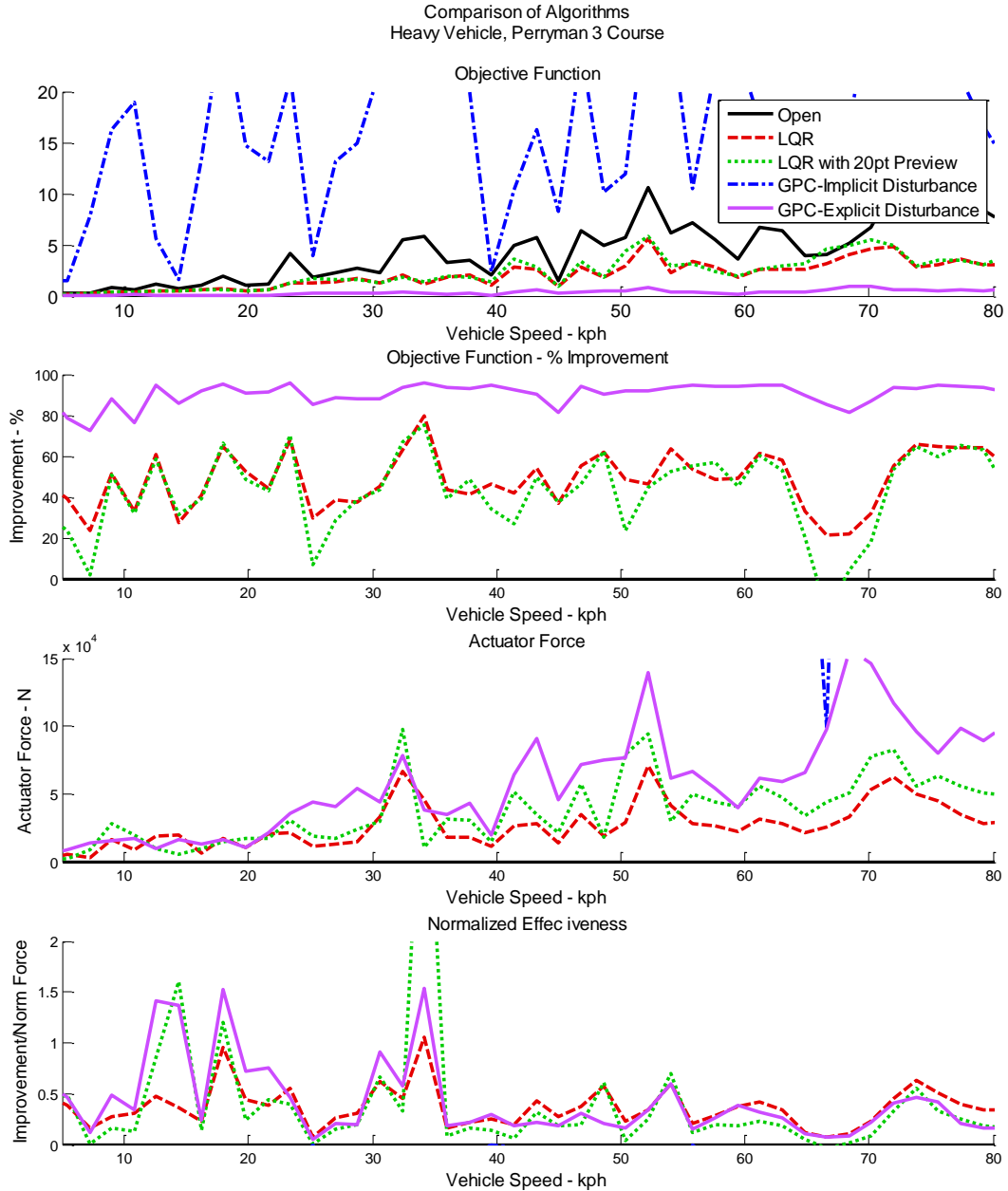
Figure 13. Comparison of control algorithms for *Heavy Vehicle* parameters on Perryman 3 course.

The quarter-car model assumed that the internal states were available for feedback control. Several of these states are not good choices for optimal control or practical implementation. For instance, tire height above the starting reference point skews the objective function for a step input and chassis vertical velocity is difficult to measure.

6.2 Preview Horizon

Preview control requires knowledge of future disturbances. These future disturbances can be measured or modeled (*6*). Figure 14 shows the effects of increasing the preview horizon from 0

(basic LQR algorithm) to 100 points. Very few preview points are required to achieve large reductions in the objective function; large numbers of preview points do not improve the performance. This corresponds well with the results reported by El Madany (*2*)**.**
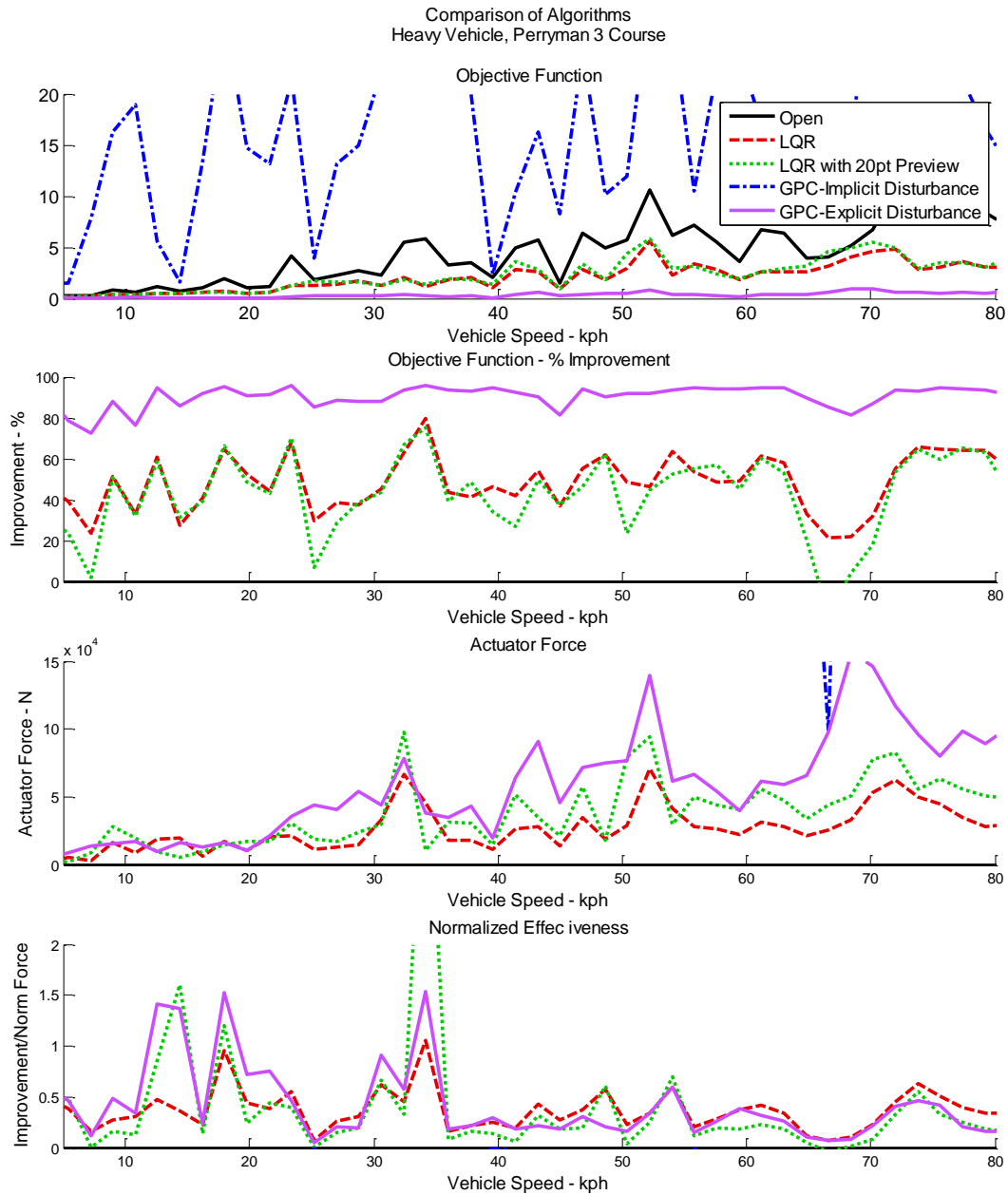

Figure 14. Comparison of effect of preview horizon on LQR.

Practical sensors to measure this value do not exist outside of a controlled laboratory. No effort was made to identify and model a sensor to directly gather disturbance data or preview data. All measurements assumed no noise or offset-bias.

6.3   System Identification

The LQR formulation requires complete and perfect knowledge of the vehicle model and internal states prior to calculation of the control laws. While this is not practical for most applications, it does provide a common algorithm to compare during simulation. This limitation can be mitigated with the Linear Quadratic Gaussian (LQG) formulation, which includes a Kalman filter to adjust an imperfect vehicle model. This is not considered in the scope of this currently reported research effort.

Generalized Predictive Control algorithm relies on a system identification to generate control laws. Typically, a given system identification is valid over a small frequency range about the primary excitation frequency of the disturbance. The robustness of the system identification was evaluated for different types of model disturbances. Figures 15 and 16 show the effects of system identifications under different disturbance types.

As shown in figure 15, GPC with Implicit Disturbances generates control laws that are valid over a range of 20 Hz and the valid range shifts with the System Identification disturbance frequency. Surprisingly, when GPC with Implicit Disturbances generates control laws with disturbances composed of multiple frequencies (either white "noise" or a signal composed of 1, 5, 7, 11, and 17 Hertz), the control laws are not valid over the entire frequency range. This suggests that new system identifications are required at higher vehicle speeds.
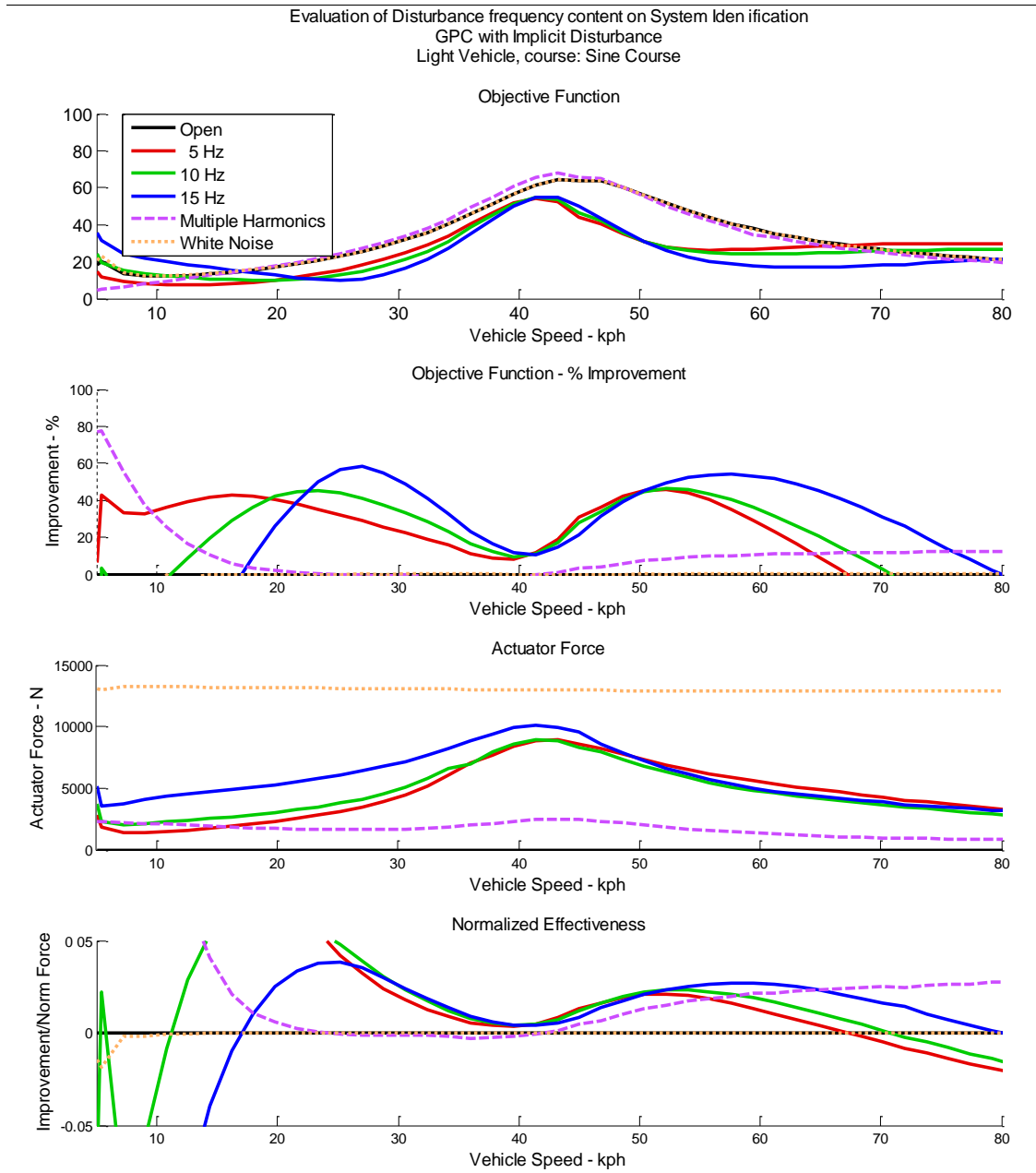
Figure 15. Comparison of effect of frequency content of disturbance for GPC with implicit disturbances system identification.

The performance of GPC with Explicit Disturbance, as shown in figure 16, improves with the addition of white "noise" or composite disturbances. In each case, it is assumed that the actuator excitation and disturbances are completely known (no noise).
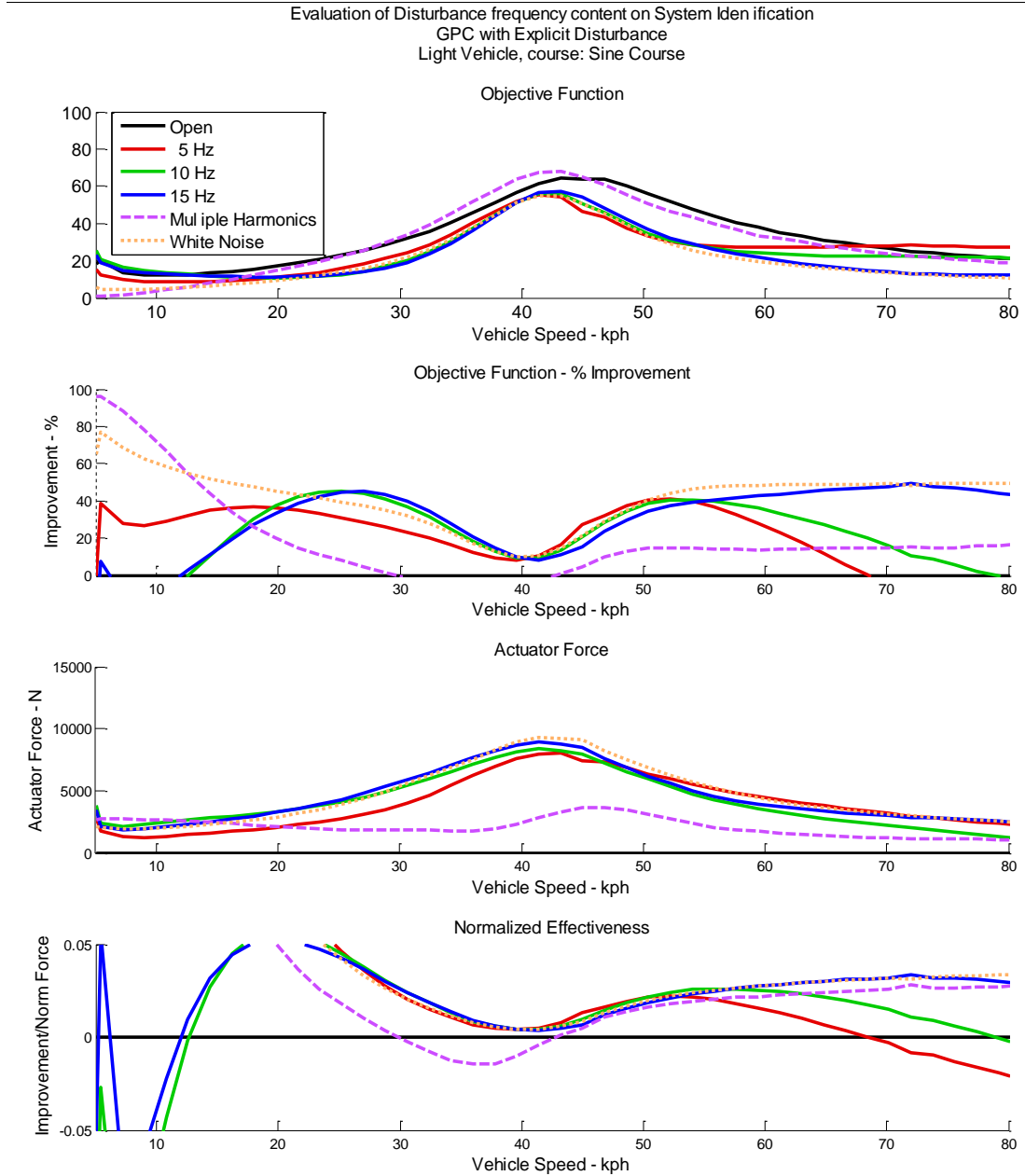
22

Figure 16. Comparison of effect of frequency content of disturbance for GPC with explicit disturbances system identification.

The weakness of GPC with Implicit Disturbances can be overcome by performing real-time system identification at new operating speed. A new system identification can be performed while the control system is already in closed-loop. This allows the algorithm to use a control law optimized over the current operating range. This approach will outperform GPC with Explicit Disturbances with a given periodic disturbance as shown in figure 17.
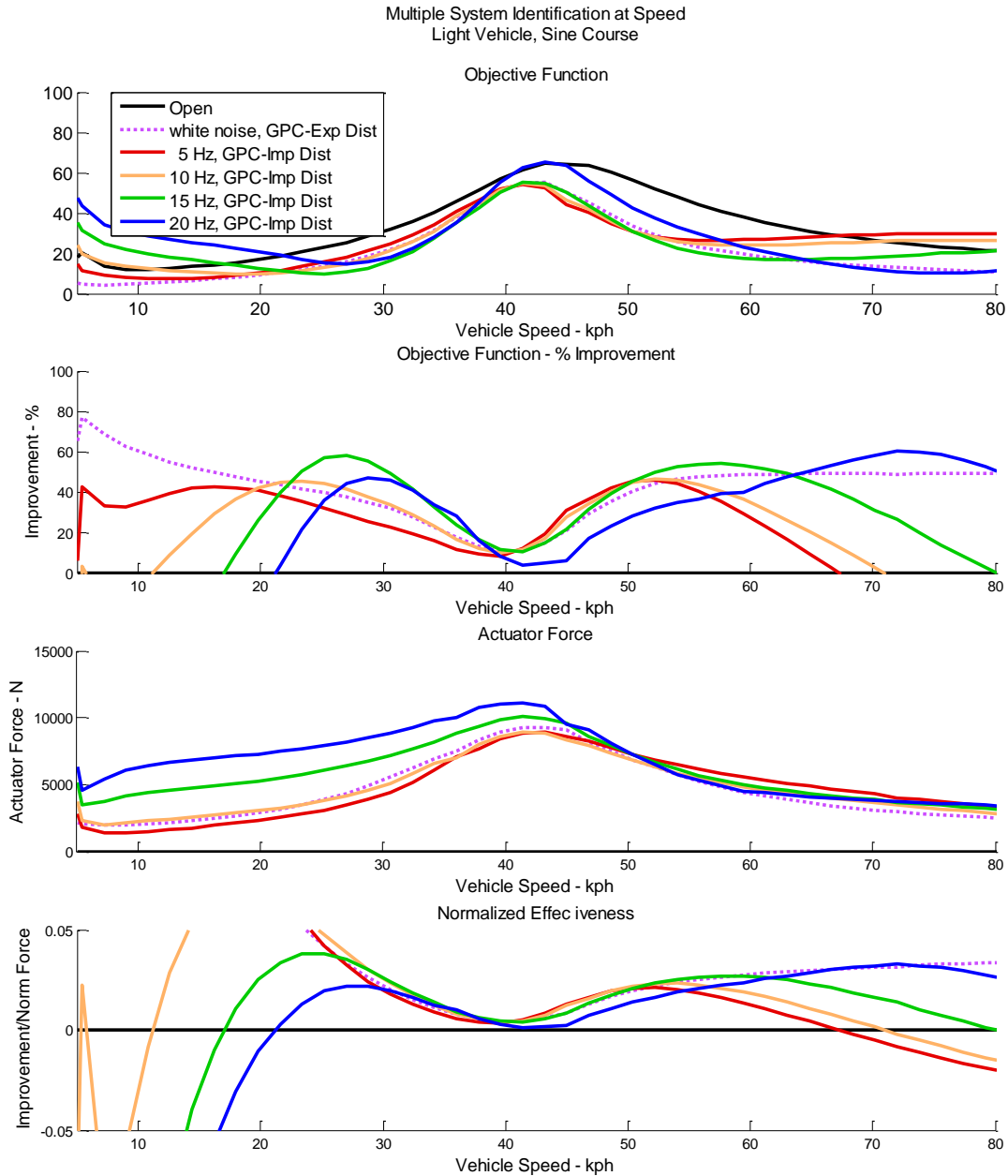
Figure 17. Effects of multiple system identifications for GPC with implicit disturbance of closed loop system in real-time.

6.4   Control Weighting

As shown in figures 18, 19, 20, and 21, when the improvement of the objective function is normalized by the actuator force, the variation of the weighting factors, (Q and R), does not greatly affect the performance of an algorithm. This property is used to compare the effectiveness of the different algorithms despite variations in actuator forces, sensor magnitudes, and weighting factors. This statement is not valid when the control laws are unable to control the system.
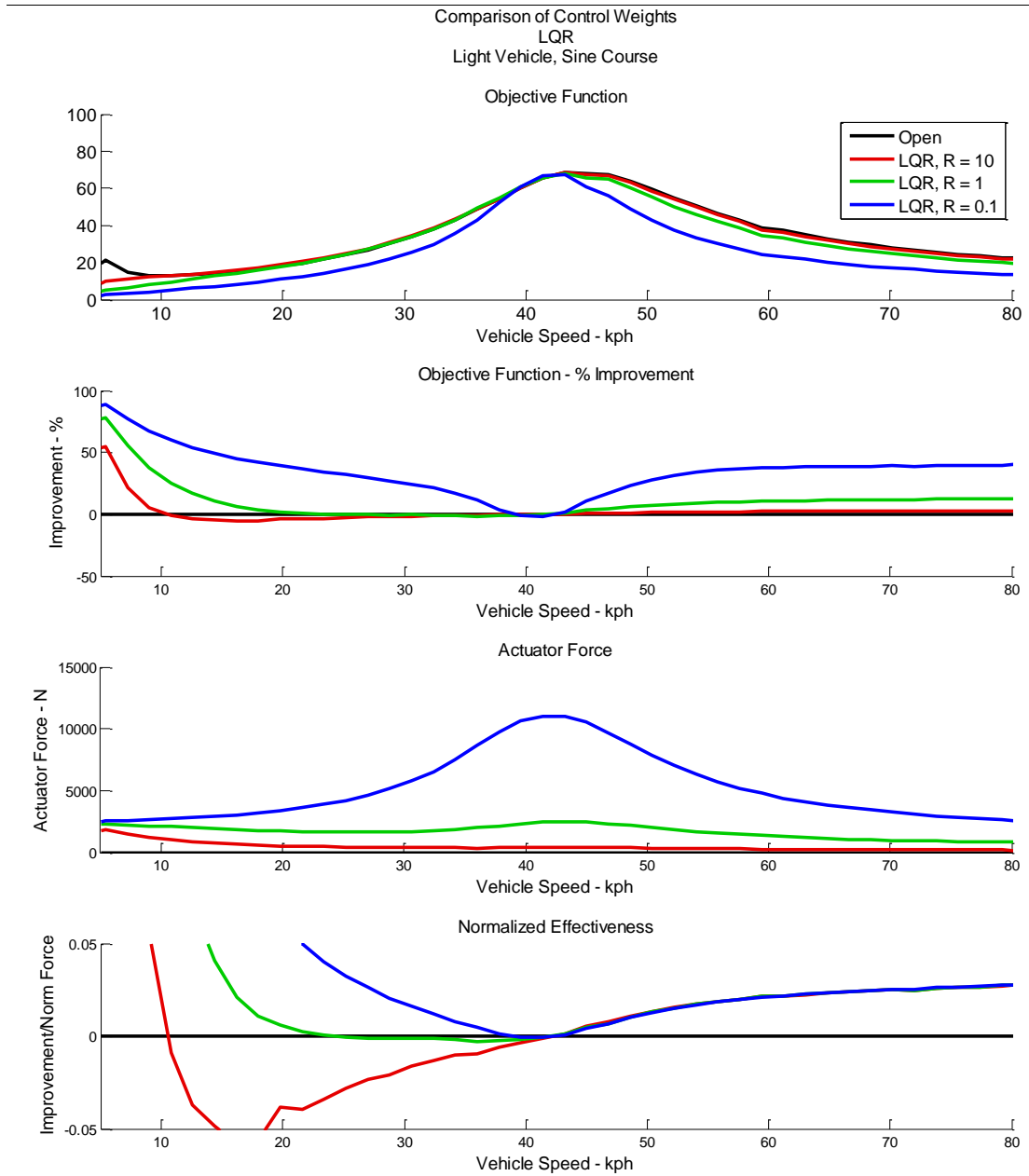
24

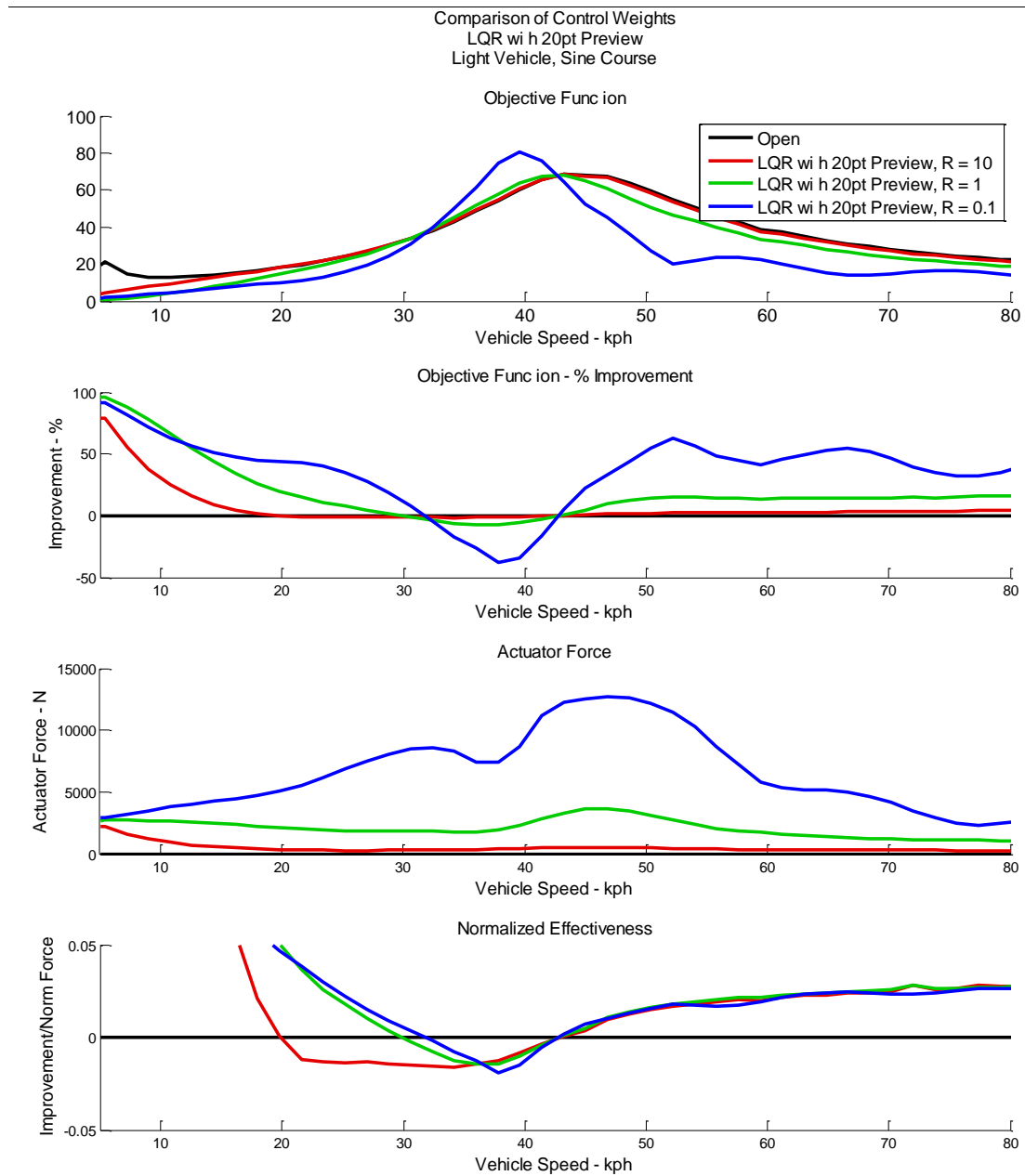Figure 18. LQR algorithm at various control weights.

Figure 19. LQR with 20 point preview control at various control weights.
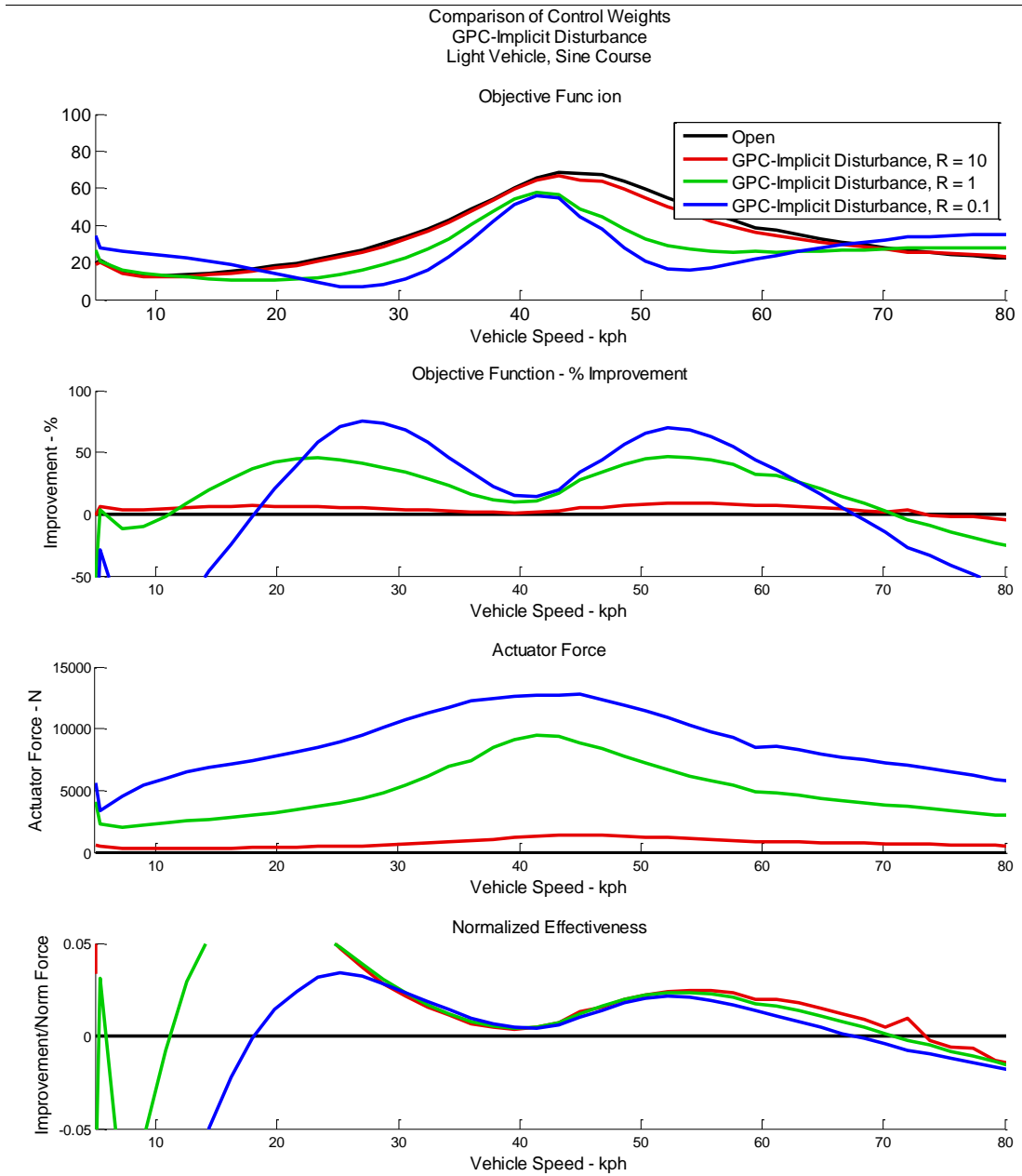
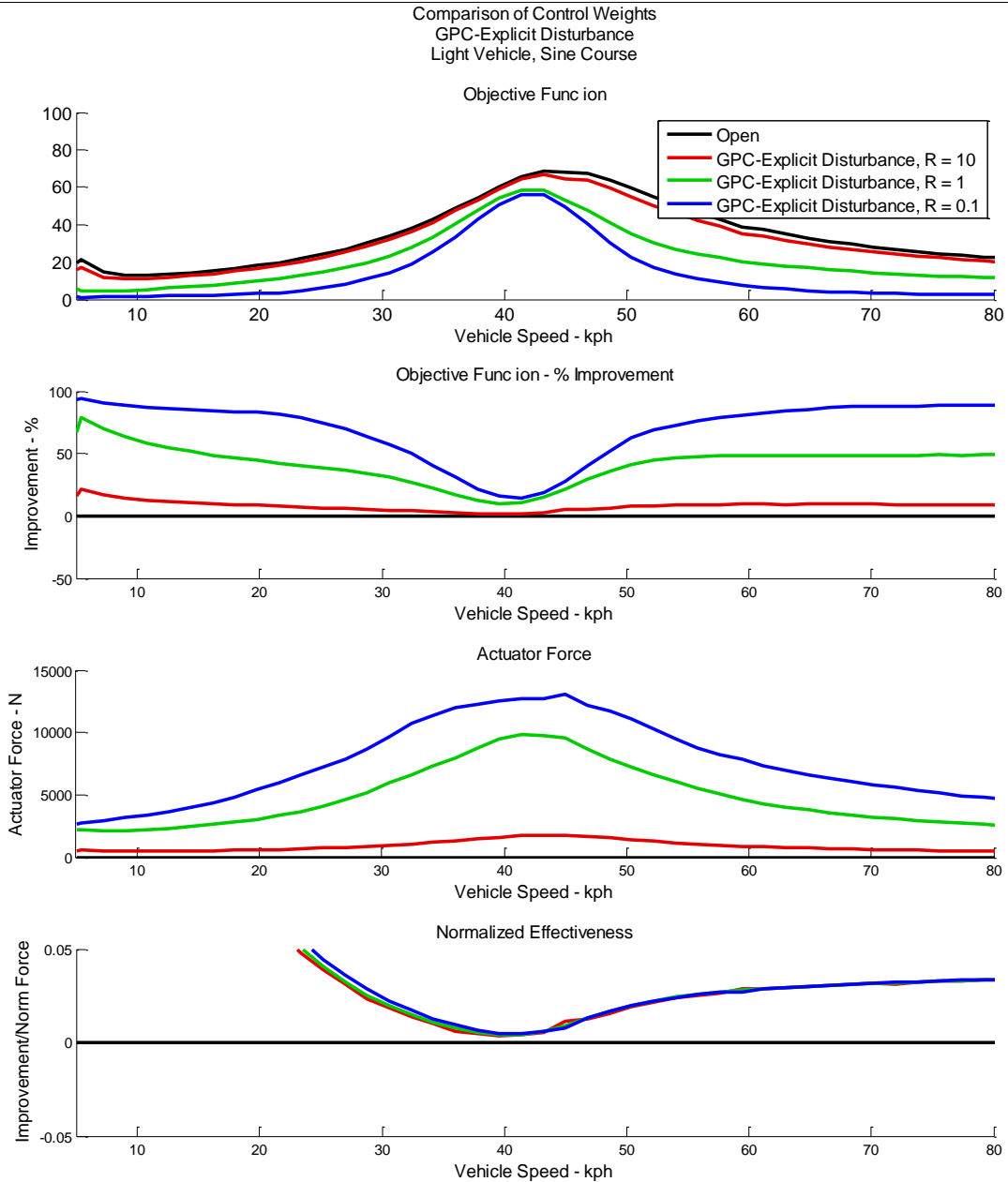Figure 20. GPC with implicit disturbances at various control weights.

Figure 21. GPC with explicit disturbances at various control weights.

7. Conclusions

Knowledge of the disturbance clearly shows an improvement in the performance of the control laws. Both LQR with Preview Control and GPC with Explicit Disturbances outperform the versions of the algorithms without disturbance knowledge. A relatively short distance of preview disturbance is required to show improvements. Longer distance preview distances do not

improve performance much. It is shown that, for a given algorithm, the control weights reduce sensor objective function at the same rate that it increases actuator objective function. Therefore, control weights can be normalized for comparison across algorithms. Though control laws based on GPC with Implicit Disturbance were valid over a very narrow speed range; the system can be re-identified periodically to achieve the best performance of all of the algorithms.

8. Future Work

Generalized Predictive Control with Explicit Disturbances will be extended to include Preview Control, and non-linear system identification will be incorporated to allow for semi-active suspension system development. These controllers will be implemented on high fidelity multi-body dynamics models and will be experimentally evaluated on a physical suspension test rig.

A two-degree-of-freedom suspension test rig has been fabricated, as shown in figure 22. This will be used to validate aspects of the control laws in hardware-in-the-loop control. This test rig has variable sprung and unsprung masses of up to 250 kg, representing a 1000 kg vehicle. The tire and suspension components can be reconfigured using commercial-off-the-shelf components or custom components as needed.

Figure 22. 2 DOF suspension test rig.
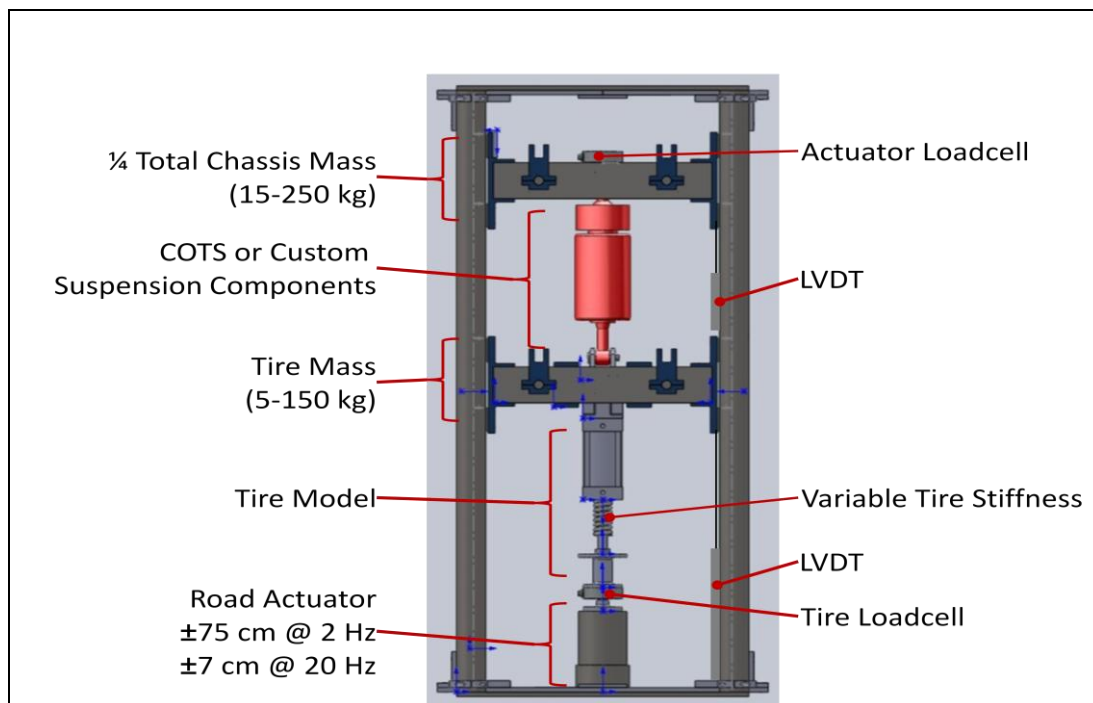
9. References

1. Bender, E. K. Optimum Linear Preview Control with Application to Vehicle Suspension. *AMSE Journal of Basic Engineering* **1968**, *90*.

2. El Madany, M. M.; Abduljabbar, Z.; Foda, M. Optimal Preview Control of Active Suspensions with Integral Constraint. *Journal of Vibration and Control* **2003**, *9*, 1377–1400.

3. van de Aa, M.A.H. Control Concept for a Semi-Active Suspension with Preview Using a Continuously Variable Damper. *Eindhoven University of Technology, Mechanical Engineering Report WFW 94.017*, 1994.

4. Kvaternik, R. G.; Juang, J. N.; Bennett, R. L. *Exploratory Studies in Generalized Predictive Control for Active Aeroelastic Control of Tiltrotor Aircraft*; NASA/TM-2000-210552; 2000.

5. Juang, J. N. Applied System Identification; PTR Prentice Hall: Edgewood Cliffs, NJ, 1994.

6. Kvaternik, R. G.; Eure, K. W.; Juang, J. N. *Exploratory Studies in Generalized Predictive Control for Active Gust Load Alleviation*; NASA/TM-2006-214296; 2006.

List of Symbols, Abbreviations, and Acronyms

2 DOF	two-degree-of-freedom
A	state-space state matrix
accent −	approximated value
accent −	first row of Markov coefficient matrix
accent ·	first derivative with respect to time
accent ··	first derivative with respect to time
ARE	Algebraic Riccati Equation
ARL	U.S. Army Research Laboratory
ARX	Autoregressive with Exogenenous
B	state-space control input matrix
C	damper coefficient
d	external disturbance vector
F	external control force
GPC	Generalized Predictive Control
J	objective function
K	spring Constant
K	Feedback Gain Matrix
LQG	Linear Quadratic Gaussian
LQR	Linear Quadratic Regulator
m	mass
MR	magneto-rheological
N	cross-coupled weighting matrix
P	solution to Algebraic Riccati Equation
Q	response weighting matrix
R	control command weighting matrix
subscript c	property of control command
subscript d	property of external disturbance

subscript S	property of sprung or chassis mass
subscript t	property of current time step
subscript U	property of unsprung or tire mass
superscript T	matrix transpose
t	current time step
u	control command vector
VTD	Vehicle Technology Directorate
x	state vector
y	measured response vector
z	element of internal state vector
α	Markov response coefficient matrix
β	Markov control coefficient matrix
δ	Markov disturbance coefficient matrix
τ	Markov future command coefficient matrix

NO. OF COPIES	ORGANIZATION	NO. OF COPIES	ORGANIZATION

INTENTIONALLY LEFT BLANK.